

# Couplings of light $I = 0$ scalar mesons to simple operators in the complex plane

B. Moussallam

*Groupe de Physique Théorique, IPN  
Université Paris-Sud 11, F-91406 Orsay, France*

June 18, 2013

## Abstract

The flavour and glue structure of the light scalar mesons in QCD are probed by studying the couplings of the  $I = 0$  mesons  $\sigma(600)$  and  $f_0(980)$  to the operators  $\bar{q}q$ ,  $\alpha_s G^2$  and to two photons. The Roy dispersive representation for the  $\pi\pi$  amplitude  $t_0^0(s)$  is used to determine the pole positions as well as the residues in the complex plane. On the real axis,  $t_0^0$  is constrained to solve the Roy equation together with elastic unitarity up to the  $K\bar{K}$  threshold leading to an improved description of the  $f_0(980)$ . The problem of using a two-particle threshold as a matching point is discussed. A simple relation is established between the coupling of a scalar meson to an operator  $j_S$  and the value of the related pion form-factor computed at the resonance pole. Pion scalar form-factors as well as two-photon partial-wave amplitudes are expressed as coupled-channel Omnès dispersive representations. Subtraction constants are constrained by chiral symmetry and experimental data. Comparison of our results for the  $\bar{q}q$  couplings with earlier determinations of the analogous couplings of the lightest  $I = 1$  and  $I = 1/2$  scalar mesons are compatible with an assignment of the  $\sigma$ ,  $\kappa$ ,  $a_0(980)$ ,  $f_0(980)$  into a nonet. Concerning the gluonic operator  $\alpha_s G^2$  we find a significant coupling to both the  $\sigma$  and the  $f_0(980)$ .

## 1 Introduction:

Exotic hadrons in QCD remain poorly understood theoretically. The recent discoveries of the  $X$ ,  $Y$ ,  $Z$  states [1], for instance, in the charmonium spectroscopy was rather unexpected. Many of the expected states, on the other hand, which are associated with gluonic excitations like hybrids or glueballs have not been unambiguously identified. The  $0^{++}$  glueball is the lightest stable particle in the QCD spectrum

in the limit where all quark masses are sent to infinity. In this situation, its mass has been computed rather accurately in quenched lattice QCD simulations [2] to be slightly smaller than two GeV. In the presence of finite quark masses, the properties of the glueball should remain relatively undisturbed provided  $m_q \gtrsim 1$  GeV. In the physical situation, however, three quarks are substantially lighter than 1 GeV. Unquenched lattice simulations have been performed but the results are somewhat contradictory. The simulations of ref. [3] obtain near to maximal mixing between glueball and  $\bar{q}q$  states and find that unquenching leads to a strong lowering of the masses. A similar effect of unquenching was observed for the  $I = 1$  scalar mesons by several groups (e.g. [5, 6]). This picture, however, is not confirmed by the recent results from ref. [4] based on unquenched simulations with  $N_f = 2 + 1$  and larger statistics who find glueball states very similar to the quenched ones.

A possible scenario, suggested from using Laplace sum rules [7, 8]<sup>1</sup> is that there could be two mesons below 2 GeV with large glueball overlap. One of these could be rather light and possibly identified with the  $\sigma(600)$ . Phenomenological implications of this scenario have been discussed in some detail in ref. [10].

The classification of the lowest lying experimentally observed scalar mesons into a flavour nonet is also not a completely solved problem [11]. It has been proposed, for instance, that the  $a_0(980)$  and the  $f_0(980)$  mesons could have a specific status as weakly bound  $K\bar{K}$  molecules [12]. This model simply explains their near degeneracy and their proximity to the  $K\bar{K}$  threshold. It also seems able to explain the values of the  $2\gamma$  partial widths [13]. Alternatively, it has been pointed out a long time ago that the mass pattern of the nonet below 1 GeV can be understood assuming a tetraquark flavour structure [14] (see also [15]).

The peculiarity of a nonet composed of the  $\sigma$ ,  $\kappa$ ,  $a_0(980)$  and  $f_0(980)$  is most clearly formulated in terms of 't Hooft's large  $N_c$  limit of QCD [16]. The masses, for instance, strongly deviate from the ideal mixing pattern predicted in this limit<sup>2</sup>. This implies that in discussing the light scalars, effects which are sub-leading in  $1/N_c$ , such as meson loops, ought to be taken into account. Modellings of meson loops effects can be found in the classic papers [18, 19]. More recently, a model from which an explicit  $1/N_c$  dependence can be deduced has been proposed [20]. Investigations in the ADS/CFT modelling of large  $N_c$  QCD have also been performed [21].

Experiments on radiative decays of the  $\phi$  meson have been proposed [22] in order to clarify the flavour structure of the light scalars. Such experiments have been performed and are planned to continue (see [23] for a review). The simplest way, however, to quantify the various aspects of the structure of the scalar resonances

---

<sup>1</sup>references to more recent work which incorporate, in particular, more realistic modelling of instanton effects can be traced e.g. from ref. [9]

<sup>2</sup>In principle, dual ideal mixing is possible [15]. The scalars must then be either tetraquarks, i.e. exotics, or else the mass squared of the  $\sigma$ -meson must be a decreasing function of the strange quark mass [17] which is unphysical.

would be via their couplings to a set of simple operators. The glue content, for instance, is best probed from the coupling to the gluonic operator  $\alpha_s G^2$ . Similarly, the  $\bar{q}q$  content is probed by the couplings of the scalar mesons to quark-antiquark operators. Such couplings have been considered for the  $I = 1$  and  $I = 1/2$  scalars by Maltman [24] who suggested that their values can also be used for properly identifying the nonet. A lattice QCD result for the coupling of  $I = 1$  scalars to  $\bar{u}d$  is presented in [25]. Studies of couplings to tetraquark operators have also been recently undertaken [26, 27].

The  $\sigma(600)$  resonance is very unstable and does not give rise to a usual Breit-Wigner behaviour in cross-sections. Its existence has been demonstrated only recently [28] by making a combined use of experimental data and theoretical properties of the  $\pi\pi$  scattering amplitude, which can be encoded into the set of Roy [29] integral equations. On the real axis, where the additional constraint of unitarity applies, the Roy equations were known as a powerful tool for analyzing experimental pion-pion scattering data [30, 31]. New high precision experimental data on low energy pion-pion scattering [32, 33, 34, 35, 36] have spurred renewed interest in these equations [37, 38, 39, 40, 41]. In ref. [38], the Roy equations are treated as a boundary value problem and exact solutions have been searched for numerically below a matching point  $\sqrt{s_A} = 0.8$  GeV.

When applied to resonances, the Roy equations are used for computing the partial-wave amplitude for complex values of the energy. The masses and widths of the resonances may be identified from the poles of the amplitude on the second Riemann sheet. The domain of validity of the Roy equations, as displayed in ref. [28] allows one to discuss both the  $\sigma$  and the  $f_0(980)$ . The same poles which appear in the elastic scattering amplitude can be shown to also appear in two-point correlation functions of scalar operators and also in  $\pi\pi$  matrix elements of these operators. The poles also appear in scattering amplitudes with a pion pair in the final state like  $\gamma\gamma \rightarrow \pi\pi$ . The residues of the poles are also determined and can be interpreted in terms of couplings between scalar resonances and operators. In the present work we consider, from this point of view, the couplings of the scalar  $I = 0$  mesons  $\sigma$  and  $f_0(980)$  to the gluonic operator  $\alpha_s G^2$  and to the quark operators  $\bar{u}u + \bar{d}d$  and  $\bar{s}s$ . We will update the results that can be obtained for these couplings using the Roy equations combined with low-energy constraints from chiral symmetry. We will also consider the couplings to two photons, which were discussed in a similar framework in ref. [42]. In that case, chiral constraints can be used as well as recent experimental data from the Belle collaboration [43, 44].

The plan of the paper is as follows. We begin in sec. 2 by constructing solutions to the Roy equations in a domain which extends up to the  $K\bar{K}$  threshold. This domain covers most of the  $f_0$  effect on the real axis. We find that a very simple generalisation of the parametrisations used in ref. [38] is adequate for approximating the solutions. In sec. 3 we use these solutions inside the Roy integral representations

to perform extrapolations to the complex energy plane. We determine the resonance poles and their associated residues (sec. 3). These results are applied in sec. 4 to the determination of the scalar mesons couplings to two photons. For this purpose, we use the coupled-channel dispersive Omnès representation for  $\gamma\gamma \rightarrow \pi\pi, K\bar{K}$  and the chirally constrained fits performed in [45]. The couplings of the scalar mesons to operators are finally considered in sec. 5. A complex plane definition is proposed from which a simple relation is obtained between the couplings and pion scalar form-factors computed at the resonance pole positions. Evaluations are made possible in this case by using chiral constraints for the form-factors in combination with coupled-channel Omnès representations [46].

## 2 Roy equation solution for $t_0^0(s)$ up to the $K\bar{K}$ threshold

In order to improve the determination of the  $f_0(980)$  properties, we begin in this section by constraining the  $I = 0$   $S$ -wave amplitude  $t_0^0(s)$  to satisfy the Roy equation up to the  $K\bar{K}$  threshold<sup>3</sup>. The Roy equation reads

$$\begin{aligned} \text{Re } t_0^0(s) = & a_0^0 + \frac{s - 4m_\pi^2}{12m_\pi^2} (2a_0^0 - 5a_0^2) \\ & + \frac{1}{\pi} \int_{4m_\pi^2}^{\infty} ds' \left[ \text{Im } t_0^0(s') \left( \frac{1}{s' - s} + K_0(s', s) \right) \right. \\ & \left. + \text{Im } t_1^1(s') K_1(s', s) + \text{Im } t_0^2(s') K_2(s', s) \right] + d_0^0(s) \end{aligned} \quad (1)$$

where  $a_0^0, a_0^2$  are the  $I = 0, 2$   $S$ -wave scattering lengths. Detailed expressions for the kernels  $K_a(s', s)$  and the driving term  $d_0^0(s)$  can be found in ref. [38]. Eq. (1) is supplemented with the non-linear, unitarity relation involving the inelasticity parameter  $\eta_0^0(s)$

$$|1 + 2i\sigma_\pi(s)t_0^0(s)| = \eta_0^0(s) \quad (2)$$

with  $\sigma_\pi(s) = \sqrt{1 - 4m_\pi^2/s}$ . The inelasticity parameter  $\eta_0^0$  is rigorously equal to one in the region  $s \leq 16m_\pi^2$ . Based on experimental indications, we use here the approximation  $\eta_0^0(s) = 1$  up to the  $s = 4m_K^2$ . Furthermore in eq. (1), we use for the  $P$ -wave  $\text{Im}(t_1^1)$  as well as the  $I = 2$  partial-wave  $\text{Im}(t_0^2)$  inputs taken from ref. [38] i.e. satisfying the coupled Roy equations below 0.8 GeV and taken from experiment above. Imaginary parts of higher partial-waves, which enter into the driving term  $d_0^0$  are also taken from experiment.

---

<sup>3</sup>We neglect isospin breaking and take  $m_K = (m_{K^+} + m_{K^0})/2$

## 2.1 Multiplicity of the solutions:

Taking the matching point as  $s_m = s_K = 4m_K^2$ , the Roy equation (1) admits a family of solutions [47, 48, 49] rather than a unique one. We will assume that the phase-shift at the  $K\bar{K}$  threshold satisfies

$$\pi < \delta_K < \frac{3\pi}{2}, \quad \delta_K \equiv \delta_0^0(s_K), \quad (3)$$

which implies [47, 48, 49] a two-parameter family of solutions<sup>4</sup>. In other terms, we must impose two conditions in order to select a unique solution. As one condition, we can fix the value of the phase-shift at one energy, for instance the value of

$$\delta_A \equiv \delta_0^0(s_A), \quad \sqrt{s_A} = 0.8 \text{ GeV}. \quad (4)$$

In order to define a second condition, we consider the singularity of the derivative of the phase-shift at the matching point. For a generic Roy solution, the divergence depends on the value of the phase-shift at the matching point in the following way [47, 49]

$$\left. \frac{d}{ds} \delta_0^0(s) \right|_{s \rightarrow s_m^-} \sim (s_m - s)^{\alpha-1}, \quad \alpha = \frac{2\delta_0^0(s_m)}{\pi} - 2. \quad (5)$$

In our case, the matching point coincides with a two-particle threshold, we expect the derivative of the phase-shift to exhibit a square-root singularity

$$\left. \frac{d}{ds} \delta_0^0(s) \right|_{s \rightarrow s_K^-} = A (s_K - s)^{-\frac{1}{2}}. \quad (6)$$

This divergence is weaker than the generic matching point divergence (5) provided the threshold phase-shift is not too large,

$$\delta_0^0(s_K) < 225^\circ. \quad (7)$$

We will assume here that this condition is fulfilled. In this case, we can use as a second condition that the phase-shift behaves as in eq. (6) close to the  $K\bar{K}$  threshold. It is not difficult to work out the explicit expression for the coefficient  $A$  of the square-root singularity in eq. (6). For this purpose, let us consider the unitarity relation for  $\text{Im } t_0^0$  in the region of the  $K\bar{K}$  threshold

$$\text{Im } t_0^0(s) = \sigma_\pi(s) |t_0^0(s)|^2 + \theta(s - s_K) \sigma_K(s) |g_0^0(s)|^2 \quad (8)$$

---

<sup>4</sup> One assumes that the following set of inputs are given: the two scattering lengths  $a_0^0$ ,  $a_0^2$ , the phase-shift  $\delta_0^0(s)$  above the matching point, the inelasticity function  $\eta_0^0(s)$  and, finally, the imaginary parts of the partial-waves  $\text{Im } t_0^0(s)$  and  $\text{Im } t_{l \geq 1}^a(s)$ .

where  $g_0^0(s)$  is the partial-wave  $\pi\pi \rightarrow K\bar{K}$  amplitude with  $I = 0$ ,  $J = 0$ . The principal value integration in the Roy equation (1) generates singularities associated with discontinuities of the derivative of  $\text{Im } t_0^0(s')$ . Finite discontinuities lead to logarithmic divergences upon integration. The square-root divergence is generated from the function  $\theta(s' - s_K)\sigma_K(s')$ . Performing the integration analytically in the neighbourhood of the threshold one easily finds that

$$A = \frac{\sigma_\pi(s_K)|g_0^0(s_K)|^2}{2 \cos 2\delta_K \sqrt{s_K}}. \quad (9)$$

Once a solution is found for a given value of  $\delta_A$ , we can compute the  $\chi^2$  over the experimental data in the range  $[s_A, s_K]$  and then search for the value of  $\delta_A$  which minimises this  $\chi^2$ . In practice, the value of the phase-shift at the  $K\bar{K}$  threshold,  $\delta_K$  should be constrained by the data on both sides of the matching point. We can thus constrain both parameters  $\delta_A$  and  $\delta_K$  by fitting the experimental data using Roy equation solutions.

## 2.2 Numerical approximations to the solution

Let us denote by  $\mathcal{R}[t_0^0]$  the right-hand side of eq. (1) and by  $\epsilon(s)$  the difference between the left and right-hand sides

$$\epsilon(s) = \mathcal{R}[t_0^0](s) - \text{Re } t_0^0(s). \quad (10)$$

We construct numerical approximations to the phase-shift in the range  $4m_\pi^2 \leq s \leq 4m_K^2$  using a simple modification of the Schenk parametrisation [50] compatible with eq. (5)

$$\tan \delta_0^0(s) = \sigma_\pi(s) \left[ a_0^0 + \sum_1^N \alpha_i \left( \frac{s}{s_\pi} - 1 \right)^i \right] \frac{s_\pi - s_0}{s - s_0} \frac{\sigma^K(s_\pi) + \beta}{\sigma^K(s) + \beta} \quad (11)$$

with  $s_\pi = 4m_\pi^2$  and  $\sigma^K(s) = \sqrt{s_K/s - 1}$ . This representation involves  $N$  polynomial parameters  $\alpha_i$  plus 2 parameters  $s_0$  and  $\beta$ . The last factor generates a square-root divergence in the derivative of  $\delta_0^0$  as expected from eq. (6). In principle, the parameter  $\beta$  could be determined as a function of the known (9) coefficient  $A$  in front of the divergence. In practice, we have left it as a free parameter, adjusted such as to help approximate the solution for  $s$  close to  $s_K$  but not necessarily reproducing the exact limiting behaviour for  $s = s_K$ . We have checked that the correct order of magnitude for  $A$  is reproduced.

The  $N + 2$  parameters in eq. (11) are determined from a variational principle, by minimising the integral over the error function squared

$$\chi_R^2 \equiv \int_{4m_\pi^2}^{4m_K^2} ds' |\epsilon(s')|^2 \quad (12)$$

while fixing the two values of  $\delta_0^0(s_A)$  and  $\delta_0^0(s_K)$ . An exact solution corresponds to  $\epsilon(s)$  vanishing identically in the whole range  $[4m_\pi^2, 4m_K^2]$  and therefore to  $\chi_R^2 = 0$ . We used routines from the MINPACK library [51] to determine the parameters in eq. (11) which minimise  $\chi_R^2$ . We increased the number of parameters up to ten. With ten parameters one achieves an accuracy  $|\epsilon(s)| \lesssim 5 \cdot 10^{-4}$  below the matching point. The behaviour of the error function is illustrated in fig. 1. The figure shows that  $\epsilon(s)$  is an oscillating function which has a number of zeros approximately equal to the number of parameters in eq. (11). The figure also illustrates how the error function evolves upon increasing the number of parameters which is suggestive of a convergence towards an exact solution. The accuracy is comparable to that quoted in ref. [38] below their matching point  $s_A$ . Above the  $K\bar{K}$  threshold,  $\epsilon(s)$  increases rapidly becoming  $\simeq 10^{-1}$ . In this region, this is similar to the results quoted in refs. [38, 40].

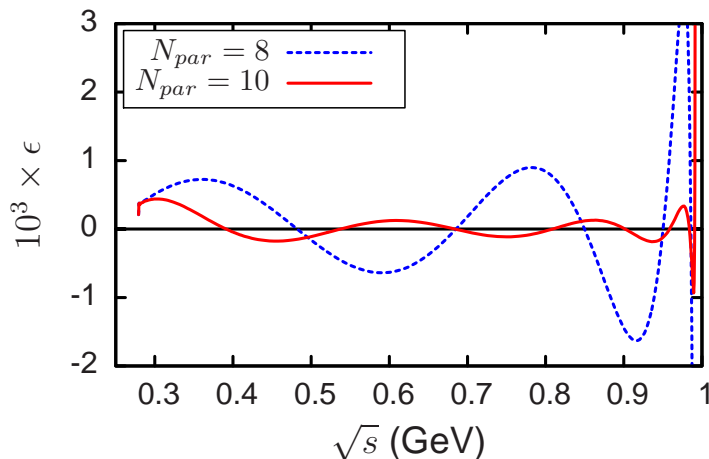


Figure 1: *Error function (see eq. (10)) corresponding to an approximation of the solution (see eq. (11)) with 8 parameters (dashed line) and 10 parameters (solid line)*

### 2.3 Inputs above the matching point:

The behaviour of the inelasticity function  $\eta_0^0(s)$  close to the  $K\bar{K}$  threshold is expected to have a strong influence on the properties of the  $f_0(980)$  resonance. By definition,  $\eta_0^0(s)$  is equal to the modulus of the  $\pi\pi \rightarrow \pi\pi$  partial-wave  $S$ -matrix element. Unitarity of the  $S$ -matrix,

$$|S_{11}|^2 = 1 - \sum_{n \neq 1} |S_{1n}|^2 \quad (13)$$

implies that  $\eta_0^0 \equiv |S_{11}|$  can be determined experimentally either a) by measuring the cross-sections of the various open inelastic channels or b) by measuring the cross-section for elastic scattering. The observation (by method (b)) that inelasticity sets in rather sharply at the  $K\bar{K}$  threshold suggests that the  $K\bar{K}$  channel should dominate the inelasticity below the  $\eta\eta$  threshold. The  $\pi\pi \rightarrow K\bar{K}$  amplitude with  $I = J = 0$  has been measured in high-statistics experiments [52, 53, 54]. We will use here the results of ref. [52] because the results of [53, 54] have been argued to necessitate some rescaling [55, 56]. The  $\pi\pi \rightarrow \eta\eta$  amplitude has been measured in ref. [57]. Some experimental information on the  $\pi\pi \rightarrow 4\pi$  inelastic amplitude is also available. We will rely on the discussion of ref. [56] who argue that the  $\pi\pi \rightarrow 4\pi$  amplitude is small in magnitude below 1.4 GeV and can be modelled by contributions from the  $f_0(1370)$  and the  $f_0(1500)$  resonances.

Fig. 2 shows the experimental determinations of  $\eta_0^0$  based on the elastic amplitude from refs [58] and [59]. The result of the  $K$ -matrix fit performed in ref. [58] is plotted (dashed curve), which is characterised by a rather deep dip near 1 GeV. We also show the central value of the fit based on the inelastic channels (solid curve). The dip, in that case, is much less pronounced. The inelastic determination of  $\eta_0^0$  is actually not inconsistent with the elastic determinations of refs. [58, 59] within the errors. It has a  $\chi^2/N = 1.6$  with the data of ref. [58] and a  $\chi^2/N = 0.4$  with the data of ref. [59] (which is smaller than one because of the very large errors). For the phase-shift  $\delta_0^0$  above the  $K\bar{K}$  threshold, we use the determination of Hyams et al. [58]. It is in good agreement with other analysis of the CERN-Munich experiment (e.g. [56]) or the analysis of the CERN-Munich-Cracow experiment [59] below 1.5 GeV. The energy region above 1.5 GeV is suppressed in the Roy equation because of the two subtractions.

### 2.4 Inputs below the matching point

In the energy range  $[s_A, 4m_K^2]$ , in which we fit the two parameters  $\delta_A$  and  $\delta_K$ , we combine the sets of data from Hyams et al. [58] and the data from Kaminski et al. [59]. The former data have much smaller error bars but it is likely that this is only because Kaminski et al. [59] have estimated their errors in a more realistic way.

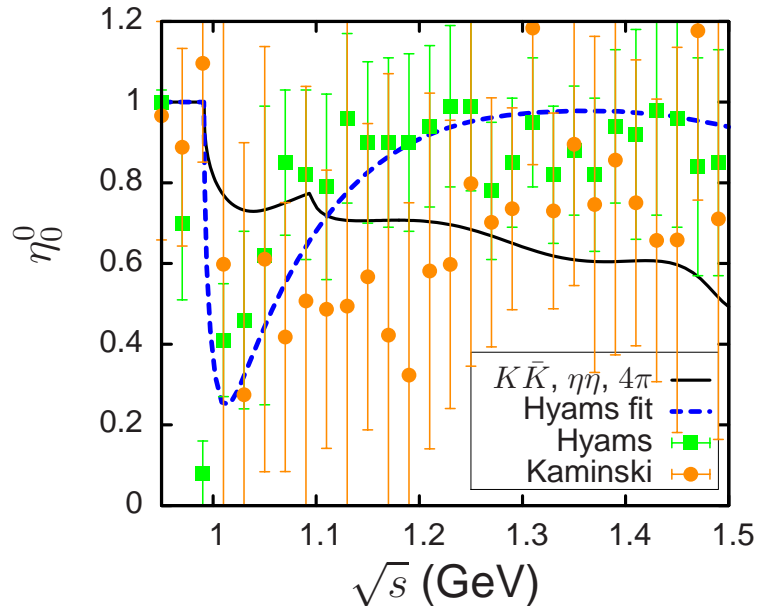


Figure 2: Inelasticity function  $\eta_0^0(s)$ . The data shown are determinations from the elastic amplitude from refs. [58] and [59]. The dashed line is the  $K$ -matrix fit from ref. [58]. The solid line is a determination of  $\eta_0^0$  based on experimental information on the inelastic channels  $K\bar{K}$ ,  $\eta\eta$  and  $4\pi$ .

This is suggested by comparing the phase-shifts resulting from different analysis of the CERN-Munich experiment (e.g. [60, 56], see also the review [61] for detailed comparisons and further experimental references). We have therefore appended a weight factor of  $1/4$  to the  $\chi^2$  of the data of Hyams et al. in the combined  $\chi^2$ . For the  $S$ -wave scattering lengths, we take the numbers quoted in the latest NA48/2 publication [36]

$$\begin{aligned} a_0^0 &= 0.2196 \pm 0.0028_{\text{stat}} \pm 0.0020_{\text{syst}} \\ a_0^2 &= -0.0444 \pm 0.0007_{\text{stat}} \pm 0.0005_{\text{syst}} \pm 0.0008_{\text{ChPT}} \end{aligned} \quad (14)$$

The results of fitting the combined data sets as described above in the region  $[s_A, 4m_K^2]$  varying the two parameters  $\delta_A$  and  $\delta_K$  are presented in table 1. We show separately the result corresponding to the two different determinations of the inelasticity function. We also show  $\hat{\chi}^2 = \chi^2/N$  (with  $N = 10$  data points) corresponding to the data of Hyams<sup>5</sup> et al. [58] and to the data of Kaminski et al. [59]. The table

<sup>5</sup>We remark that while the  $\chi^2$  seems large, half of its value comes from the single energy bin with  $E = 0.99$  GeV.

$\eta_0^0$	$\delta_A$	$\delta_K$	$\hat{\chi}_{[58]}^2$	$\hat{\chi}_{[59]}^2$
(a)	$(80.9 \pm 1.4)^\circ$	$(190_{-10}^{+5})^\circ$	2.7	1.9
(b)	$(82.9 \pm 1.7)^\circ$	$(200_{-10}^{+5})^\circ$	2.2	1.3

Table 1: Results for the two phases  $\delta_A$  and  $\delta_K$  from fitting the experimental phase-shifts in the range  $0.8 \text{ GeV} \leq \sqrt{s} \leq 2m_K$  with Roy solution functions corresponding to two different central values of the inelasticity function (see fig. 2). On the first line  $\eta_0^0$  is determined from a sum over inelastic channels (shallow-dip shape), on the second line  $\eta_0^0$  is determined from the elastic channel (deep-dip shape).

shows that a better  $\chi^2$  is obtained upon using the inelasticity function from the elastic data (deep-dip shape). This reproduces the observation first made in the recent analysis of ref. [41]. In that work, a variant of the three coupled Roy equations (derived from once-subtracted dispersion relations) have been considered in their whole domain of validity, i.e. up to  $\sqrt{s} = 1.1 \text{ GeV}$  and required to be satisfied withing the errors of the data. Their analysis favours a value for the threshold phase  $\delta_K$  somewhat larger than the results of table 1 while their result for  $\delta_A$  is compatible with ours. Fig. 3 displays the curves for the phase-shift  $\delta_0^0$  corresponding to the fit results of table 1. The figure also shows the phase-shifts from the Berkeley experiment [62] which were not included in the fit. Numerical values of the parameters describing the Roy solution phase-shifts (see eq. (11)) are given in the appendix.

### 3 Poles and residues of the $\sigma(600)$ and $f_0(980)$

Resonances correspond to poles of the  $\pi\pi \rightarrow \pi\pi$  scattering amplitude  $t_0^0(s)$  on unphysical Riemann sheets. These poles are also present in form-factors and correlation functions which involve currents which can couple to a pion pair in the  $S$ -wave. We will consider only the second Riemann sheet here and recall a few standard formulas which enable one to perform the continuations <sup>6</sup>. These formulas can be expressed in terms of the amplitude  $t_0^0(s)$ .

Let us start with the continuation of the amplitude  $t_0^0$  itself. Its right-hand cut is associated with unitarity relations and has successive thresholds in  $s$ :  $4m_\pi^2$ ,  $16m_\pi^2$ ,  $36m_\pi^2$ ,  $K\bar{K}$ ,  $\dots$ . The second sheet is defined with respect to the discontinuity relation which holds between the first two thresholds  $4m_\pi^2 \leq s \leq 16m_\pi^2$ . Using the property of real-analyticity  $t_0^0(z^*) = t_0^{0*}(z)$  (which results from  $T$ -invariance), it can be written as

$$t_0^0(s + i\epsilon) - t_0^0(s - i\epsilon) = 2\sigma^\pi(s - i\epsilon)t_0^0(s - i\epsilon)t_0^0(s + i\epsilon) \quad (15)$$

<sup>6</sup>More general formulas, for a four sheets situation can be found e.g. in ref. [63]

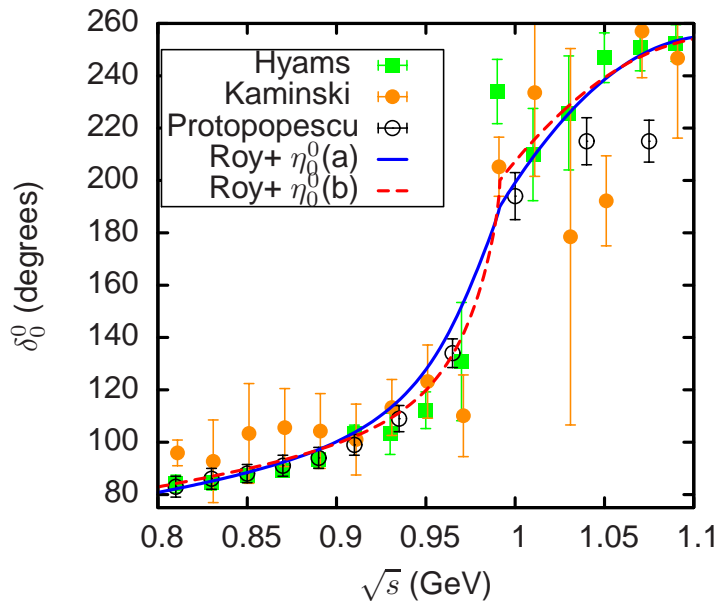


Figure 3:  $I = 0$   $S$ -wave  $\pi\pi$  phase-shifts: for  $\sqrt{s} \leq 2m_K$  the two curves represent solutions of the Roy equation corresponding to two different determinations of the inelasticity function  $\eta_0^0$  (see fig. 2).

where we have introduced

$$\sigma^\pi(z) \equiv \sqrt{4m_\pi^2/z - 1} \quad (16)$$

(which satisfies  $\sigma^\pi(s - i\epsilon) = i\sigma_\pi(s)$ ). From relation (15), one finds that the second sheet extension of  $t_0^0$  is

$$t_0^{0,II}(z) = \frac{t_0^0(z)}{1 - 2\sigma^\pi(z)t_0^0(z)} \quad (17)$$

which is easily seen to verify the continuity relation  $t_0^{0,II}(s - i\epsilon) = t_0^0(s + i\epsilon)$ .

The poles of the  $T$ -matrix can now be determined by searching for the zeros of the denominator in eq. (17):  $S_0^0(z) = 1 - 2\sigma^\pi(z)t_0^0(z)$  (which is the partial-wave  $S$ -matrix). The derivative of  $S_0^0(z)$

$$\dot{S}_0^0(z_S) \equiv \left. \frac{d}{dz}(1 - 2\sigma^\pi(z)t_0^0(z)) \right|_{z=z_S} \quad (18)$$

is needed in order to determine the residues. Numerical results for the pole positions and the  $S$ -matrix derivatives are presented in table 2. The central values in the table correspond to the Roy solution associated with the deep-dip shaped  $\eta_0^0$ . This

	$\sqrt{z_S}$ (MeV)	$\dot{S}_0^0(z_S)$ (GeV <sup>-2</sup> )
$\sigma(600)$	$(442_{-8}^{+5}) + i(274_{-5}^{+6})$	$-(0.75_{-0.15}^{+0.10}) + i(2.20_{-0.10}^{+0.14})$
$f_0(980)$	$(996_{-14}^{+4}) + i(24_{-3}^{+11})$	$-(1.1_{-0.4}^{+3.0}) + i(6.6_{-1.0}^{+0.8})$

Table 2: Positions of the complex poles and values of the corresponding derivatives of the  $S$ -matrix  $S_0^0$  from the Roy integral representation of  $t_0^0$  and the real-axis Roy solution discussed in sec. 2

choice gives a result for the  $\sigma$  position very close to that of ref. [28]. The errors were determined by varying the most significant parameters in the Roy equation i.e. the two scattering lengths  $a_0^0, a_0^2$ , the two phase-shifts  $\delta_0^0(s_A), \delta_0^0(s_K)$  (see table 1) and the parameters of the  $f_2$  meson which dominates the driving term. We have also included the result of varying between the two different determinations of the inelasticity in the form of asymmetric errors. For instance, using the shallow-dip inelasticity, the value of the sigma pole position is located at :  $\sqrt{s_\sigma} = 436 + i278$  MeV and that of the  $f_0$  is located at  $\sqrt{s_{f_0}} = 983 + i36$  MeV. The errors on the  $\sigma$  pole parameters quoted in table 2 are smaller than those in [28]: this can be traced to the fact that the range of variation for the phase  $\delta_0^0(s_A)$  as determined from the fit using Roy solutions is smaller than the one estimated in ref. [28].

## 4 Scalar meson couplings to two photons

### 4.1 $\gamma\gamma \rightarrow \pi\pi$ on the real axis:

Information on the couplings of the light scalar mesons to two photons can be extracted from the amplitudes  $\gamma\gamma \rightarrow \pi^0\pi^0, \pi^+\pi^-$ . This may be performed in a model independent way by making use of the analyticity and unitarity properties of the partial-wave amplitudes  $h_{J,\lambda\lambda'}^I(s)$  which, as a consequence, satisfy Omnès-type [64] dispersive representations. A representation of this kind for  $h_{0,++}^0(s)$  was reconsidered recently [45] which makes use of a two-channel extension of the Omnès approach [65, 66]. It should be valid in a range of energies up to one GeV where it is a reasonably good approximation to retain just two channels ( $\pi\pi, K\bar{K}$ ) in the unitarity relation. This representation involves also the  $\gamma\gamma \rightarrow K\bar{K}$  isoscalar

partial-wave amplitude  $k_{0,++}^0(s)$  and has the following form

$$\begin{aligned} \begin{pmatrix} h_{0,++}^0(s) \\ k_{0,++}^0(s) \end{pmatrix} = & \quad (19) \\ & \begin{pmatrix} \bar{h}_{0,++}^{0,Born}(s) \\ \bar{k}_{0,++}^{0,Born}(s) \end{pmatrix} + \mathbf{\Omega}(s) \times \left[ \begin{pmatrix} b^{(0)}s + b'^{(0)}s^2 \\ b_K^{(0)}s + b_K'^{(0)}s^2 \end{pmatrix} \right. \\ & + \frac{s^3}{\pi} \int_{-\infty}^{-s_0} \frac{ds'}{(s')^3(s'-s)} \mathbf{\Omega}^{-1}(s') \operatorname{Im} \begin{pmatrix} \bar{h}_{0,++}^{0,Res}(s') \\ \bar{k}_{0,++}^{0,Res}(s') \end{pmatrix} \\ & \left. - \frac{s^3}{\pi} \int_{4m_\pi^2}^{\infty} \frac{ds'}{(s')^3(s'-s)} \operatorname{Im} \mathbf{\Omega}^{-1}(s') \begin{pmatrix} \bar{h}_{0,++}^{0,Born}(s') \\ \bar{k}_{0,++}^{0,Born}(s') \end{pmatrix} \right]. \end{aligned}$$

The right-hand side of this equation involves the  $2 \times 2$  Omnès matrix  $\mathbf{\Omega}$ , which encodes the effects of the final-state interaction. Its matrix elements  $\Omega_{ij}$  are determined from the  $T$ -matrix by solving (numerically) the set of homogeneous coupled integral equations which arise from combining dispersion relations and two-channel unitarity

$$\Omega_{ij}(s) = \frac{1}{\pi} \int_{4m_\pi^2}^{\infty} \frac{ds'}{s'-s} (\mathbf{T}^*(s')\Sigma(s')\mathbf{\Omega}(s'))_{ij} \quad (20)$$

with  $\Sigma(s) = \operatorname{diag}(\sigma_\pi(s), \sigma_K(s))$ . One assumes asymptotic conditions on  $T_{ij}(s)$  (i.e. that  $T_{12}(s)$  goes to zero and that the sum of the eigen-phase shifts goes to  $2\pi$  [67]) which ensure that eqs. (20) have a unique solution once initial conditions are specified

$$\Omega_{ij}(0) = \delta_{ij} . \quad (21)$$

These asymptotic conditions are rather close from the experimental values at  $\sqrt{s} \simeq 2$  GeV. Eq. (19) also involves contributions from the left-hand cut of the partial-waves which are associated with singularities of the cross-channel amplitude  $\gamma\pi \rightarrow \gamma\pi$ . The leading singularity arises from the charged pion pole which is exactly calculable and labelled  $\bar{h}_{0,++}^{0,Born}(s')$  in eq. (19) (this term also dominates the amplitude in the soft photon limit). Singularities associated with multi-pion cuts are described more phenomenologically (but with reasonable accuracy) through the light resonance contributions, labelled  $\bar{h}_{0,++}^{0,Res}(s')$  in the above formula. Finally, eq. (19) involves four polynomial parameters. These have been introduced by writing over-subtracted dispersion relations, such as to cutoff integral contributions from higher energy regions. The polynomial parameters have been determined in ref. [45] from a chirally constrained fit<sup>7</sup> of the experimental data from ref. [43] (charged pions) and ref. [44]

---

<sup>7</sup> The fit was performed in an energy range  $\sqrt{s} \leq 1.3$  GeV. For  $I = 2$  amplitudes and for  $J = 2$  amplitudes, single channel Omnès representations were used. Chiral constraints arise upon matching the dispersive and the chiral two-loop representations [68, 69] from the fact that the  $p^4$  and certain  $p^6$  chiral coupling-constants are known.

(neutral pions). In the present work, we use the  $\pi\pi$  phase-shifts obtained by solving the Roy equation below the  $K\bar{K}$  threshold in association with the deep-dip inelasticity as discussed in sec. 2. As compared to ref. [45], this leads to small differences in the  $\gamma\gamma \rightarrow \pi\pi$  amplitudes localised in the region of the  $f_0(980)$  peak. The values of the fitted parameters and the polarisabilities are not modified.

## 4.2 $\gamma\gamma \rightarrow \pi\pi$ in the complex plane

Once the polynomial parameters are determined, the integral representations (19) (20) allow one to compute the partial-wave amplitude  $h_{0,++}^0(s)$  for complex values of  $s$ . In order to compute the second sheet extension one considers the discontinuity between the first two thresholds which reads,

$$h_{0,++}^0(s+i\epsilon) - h_{0,++}^0(s-i\epsilon) = 2\sigma^\pi(s-i\epsilon)t_0^0(s-i\epsilon)h_{0,++}^0(s+i\epsilon), \quad (22)$$

such that the second sheet extrapolation is

$$h_{0,++}^{0,II}(z) = \frac{h_{0,++}^0(z)}{1 - 2\sigma^\pi(z)t_0^0(z)}. \quad (23)$$

The quantity of interest here is the decay width of the scalar mesons into two photons. Following Pennington [70], it can be defined by first identifying the residues of the amplitudes  $t_0^{0,II}(z)$  and  $h_{0,++}^{0,II}(z)$  in terms of coupling constants

$$32\pi t_0^{0,II}(z)\Big|_{pole} = \frac{g_{S\pi\pi}^2}{z_S - z}, \quad h_{0,++}^{0,II}(z)\Big|_{pole} = \frac{g_{S\pi\pi}g_{S\gamma\gamma}}{z_S - z}. \quad (24)$$

The couplings  $g_{S\gamma\gamma}$ ,  $g_{S\pi\pi}$  are expected to be complex numbers (see below). One can formally define the decay width by taking the usual relation between a coupling constant and the corresponding decay width

$$\Gamma_{S \rightarrow 2\gamma} \equiv \frac{|g_{S\gamma\gamma}|^2}{16\pi m_S}, \quad (25)$$

which yields the following numerical results for the two-photon widths of the scalar mesons

$$\begin{aligned} \Gamma_{\sigma(600) \rightarrow 2\gamma} &= (2.08 \pm 0.20_{-0.04}^{+0.07}) \quad (\text{keV}) \\ \Gamma_{f_0(980) \rightarrow 2\gamma} &= (0.29 \pm 0.21_{-0.07}^{+0.02}) \quad (\text{keV}). \end{aligned} \quad (26)$$

The separation of the errors reflect the structure of the Omnès representation (19). The first error is associated with varying the subtraction parameters in eq. (19), i.e. it essentially reflects the experimental errors in the two-photon cross-sections.

The second error is associated with the uncertainties in the Omnès matrix elements coming from the  $\pi\pi$  phase-shifts and inelasticities. Fig. 4 compares our value for the sigma width with results quoted in the recent literature [70, 71, 72, 73, 74, 75, 76, 77] (see also [78]) which are all based on the complex pole definition. Evaluations using a Breit-Wigner definition can yield a somewhat different result (e.g. [79]). In the case of the  $f_0(980)$ , which is a rather narrow resonance, the two definitions should give reasonably compatible results. The central value which we find in (26) is practically identical to the one quoted in the PDG [80].

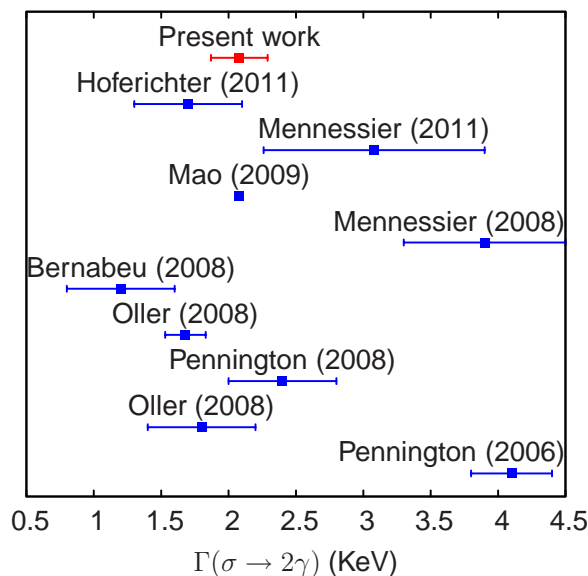


Figure 4: Recent determinations of the  $\sigma \rightarrow 2\gamma$  width from experimental measurements of  $\gamma\gamma \rightarrow 2\pi$  cross-sections.

Let us finally quote the corresponding central complex values of the coupling constants  $g_{S\gamma\gamma}$ ,  $g_{S\pi\pi}$  (in GeV),

$$\begin{aligned} g_{\sigma\gamma\gamma} &= (-0.31 + i0.60) 10^{-2}, & g_{\sigma\pi\pi} &= 1.12 + i4.63 \\ g_{f_0\gamma\gamma} &= (0.38 - i0.02) 10^{-2}, & g_{f_0\pi\pi} &= 0.23 + i2.79 . \end{aligned} \quad (27)$$

It is striking that these couplings can be far from being real. It is difficult to find a general physical interpretation for the phases of the couplings but it is instructive to consider the case of a narrow resonance, i.e. when  $\text{Im } z_S$  is small. In this situation, the Breit-Wigner approximation describes the amplitude in the region of the zero and the corresponding pole of the resonance

$$S_0^0(z) \simeq S_B(k) \frac{k - k_S}{k - k_S^*} \quad (28)$$

where  $k$  is the  $\pi\pi$  momentum,  $k = \sqrt{z/4 - m_\pi^2}$ , and  $S_B$  is a slowly varying function. Neglecting contributions which are quadratic in  $\text{Im } z_S$ , this representation gives the derivative at  $z = z_S$  as

$$\dot{S}_0^0(z_S) \simeq \frac{i \exp(2i\delta_0^0(\text{Re } z_S))}{2\text{Im } z_S} \quad (29)$$

Using this in the expressions for the residues, the coupling  $g_{S\pi\pi}$  gets expressed as

$$\frac{g_{S\pi\pi}^2}{32\pi} \simeq \frac{-\exp(-2i\delta_0^0(\text{Re } z_S))\text{Im } z_S}{\sigma_\pi(\text{Re } z_S)}, \quad (30)$$

i.e. the phase of  $g_{S\pi\pi}$  is given in terms of the phase-shift at the resonance mass

$$g_{S\pi\pi} = |g_{S\pi\pi}| e^{i(\frac{\pi}{2} - \delta_0^0(\text{Re } z_S))} \quad (31)$$

and vanishes only in the absence of any non-resonant background phase. In the case of the coupling  $g_{S\gamma\gamma}$  one finds, at leading order in  $\text{Im } z_S$ ,

$$g_{S\pi\pi}g_{S\gamma\gamma} \simeq 2i \exp(-2i\delta_0^0(\text{Re } z_S))h_0^0(\text{Re } z_S)\text{Im } z_S \quad (32)$$

i.e. (using (31))

$$\text{Phase}(g_{S\gamma\gamma}) = \text{Phase}(h_0^0(\text{Re } z_S)) - \delta_0^0(\text{Re } z_S) \quad (33)$$

which vanishes modulo  $\pi$  when  $\text{Re } z_S$  is in the region of applicability of Watson's theorem. These narrow width estimates for the phases provide a reasonably good approximation for the  $f_0(980)$  when its mass is located below the  $K\bar{K}$  threshold (which is not the case for our central value).

## 5 $\sigma(600)$ and $f_0(980)$ couplings to gluon and quark operators

### 5.1 Definitions

The  $\sigma(600)$  and  $f_0(980)$  mesons have the same quantum numbers  $J^{PC} = 0^{++}$  as the vacuum which are also those expected for the lightest glueball. One can characterise the gluon content of a scalar meson from its coupling to the gluonic operator  $\alpha_s G^2$ . One may also consider the trace of the energy-momentum tensor operator,  $\theta_\mu^\mu$ , which is proportional to  $\alpha_s G^2$  in the chiral limit. Correspondingly, two coupling constants  $C_S^{GG}$ ,  $C_S^\theta$  (with mass dimension) can be introduced

$$\begin{aligned} \langle 0 | \alpha_s G^{a\mu\nu} G_{\mu\nu}^a | S \rangle &= m_S^2 C_S^{GG} \\ \langle 0 | \theta_\mu^\mu | S \rangle &= m_S^2 C_S^\theta \end{aligned} \quad (34)$$

where  $S$  is either the  $\sigma$  or the  $f_0(980)$  meson. We will also consider matrix elements associated with scalar quark-antiquark operators. It is convenient to use a normalisation which remains well defined in the chiral limit

$$\langle 0|\bar{u}u + \bar{d}d|S\rangle = \sqrt{2}B_0 C_S^{uu}, \quad \langle 0|\bar{s}s|S\rangle = B_0 C_S^{ss}. \quad (35)$$

with  $B_0 = -\lim_{m_q \rightarrow 0} \langle 0|\bar{q}q|0\rangle/F_\pi^2$ . With this convention, the couplings are renormalisation group invariant in the chiral limit.

At first, it is necessary to clarify the meaning of such matrix elements since scalar mesons are resonances and not stable one-particle states. One may use a complex plane definition, which is rather natural here as it applies equally well to broad resonances like the  $\sigma$  or to ordinary narrow resonances. A simple relation between the couplings  $C_S^j$  and pion scalar form-factors can be derived. For this purpose, let us consider two-point correlation functions

$$\Pi_{jj}(s) = i \int d^4x e^{ipx} \langle 0|T j_S(x) j_S(0)|0\rangle \quad (36)$$

where  $j_S(x)$  is one of the scalar operators considered above. The correlator  $\Pi_{jj}$  satisfies a Källén-Lehmann representation (e.g. [81])

$$\Pi_{jj}(s) = \frac{s^3}{2\pi} \int_{4m_\pi^2}^{\infty} ds' \frac{\rho_{jj}(s')}{(s')^3(s'-s)} + \alpha s^2 + \beta s + \gamma \quad (37)$$

(written here with three subtractions) in which the spectral function is given as a sum over a complete set of states

$$(2\pi)^4 \sum_n \delta^4(p_n - q) |\langle 0|j_S(0)|n\rangle|^2 = \theta(q_0) \rho_{jj}(q^2). \quad (38)$$

The discontinuity of  $\Pi_{jj}$  across the real axis in the range  $4m_\pi^2 \leq s \leq 16m_\pi^2$  is generated by the two-pion states  $n = \pi^a \pi^a$  in the sum (38) and it can be written as

$$\Pi_{jj}(s+i\epsilon) - \Pi_{jj}(s-i\epsilon) = \frac{3}{16\pi} \sigma^\pi(s-i\epsilon) F_j(s-i\epsilon) F_j(s+i\epsilon). \quad (39)$$

Here,  $F_j$  is the form-factor associated with the two-pion matrix element of  $j_S$

$$\langle 0|j_S(0)|\pi^i(p)\pi^j(p')\rangle = \delta^{ij} F_j((p+p')^2). \quad (40)$$

In deriving eq. (39) one makes use of the fact that  $F_j(s)$  is itself a real-analytic function. It has a cut along the positive real axis, and its discontinuity in the range  $[4m_\pi^2, 16m_\pi^2]$  reads

$$F_j(s+i\epsilon) - F_j(s-i\epsilon) = 2\sigma^\pi(s-i\epsilon) t_0^0(s-i\epsilon) F_j(s+i\epsilon). \quad (41)$$

From the discontinuity relations (39) (41), it is simple to deduce the second sheet extensions of the form-factor

$$F_j^{II}(z) = \frac{F_j(z)}{1 - 2\sigma^\pi(z)t_0^0(z)} \quad (42)$$

and that of the correlator  $\Pi_{jj}$

$$\Pi_{jj}^{II}(z) = \Pi_{jj}(z) + \frac{3}{16\pi} \frac{\sigma^\pi(z) (F_j(z))^2}{1 - 2\sigma^\pi(z)t_0^0(z)}. \quad (43)$$

These expressions show that the form factor and the correlation function on the second Riemann sheet have exactly the same poles  $z_S$  as the  $T$ -matrix. Considering the residue of the pole provides a natural identification for the resonance couplings  $\langle 0|j_S|S\rangle$ ,

$$\Pi_{jj}^{II}(z)|_{pole} \equiv \frac{(\langle 0|j_S|S\rangle)^2}{z_S - z}, \quad (44)$$

which thus get expressed in terms of the  $\pi\pi$  form-factor evaluated at the position of the pole,

$$\langle 0|j_S|S\rangle = \sqrt{\frac{-3\sigma^\pi(z_S)}{16\pi \dot{S}_0^0(z_S)}} F_j(z_S). \quad (45)$$

One can verify that the interpretation of residues in terms of coupling constants satisfy consistency conditions. For instance, one expects the residue of the form-factor  $F_j^{II}(z)$  to involve the product of the two couplings  $\langle 0|j_S|S\rangle$  and  $g_{S\pi\pi}$  in the following way

$$F_j^{II}(z)|_{pole} = \frac{\langle 0|j_S|S\rangle \times g_{S\pi\pi}}{\sqrt{3}(z_S - z)}. \quad (46)$$

It is easy to verify that this expression can be exactly recovered using formulas (17),(42), (43) for the second-sheet extensions together with the definition of  $g_{S\pi\pi}$  from the residue of  $t_0^{0,II}(z)$  and the definition of  $\langle 0|j_S|S\rangle$  from the residue of  $\Pi_{jj}^{II}(z)$ .

In the limit of narrow resonances, one can express the couplings  $C_S^j$  in terms of the form-factor  $F_j$  evaluated on the real axis. For this purpose, one can write  $F_j$  in the neighbourhood of the resonance position as a function of the momentum  $k$

$$F_j(z) = \frac{\phi_j(k)}{k - k_S^*} \quad (47)$$

displaying explicitly the pole on the second sheet. If the pole is close to the real axis we can expand the function  $\phi_j(k)$ ,

$$\phi_j(k_S) = \phi_j(\text{Re } k_S) + i(\text{Im } k_S)\phi'(\text{Re } k_S) + \dots \quad (48)$$

which, to lowest order in  $\text{Im } k_S$  leads to the approximation

$$F_j(z_S) \simeq \frac{1}{2} F_j(\text{Re } z_S) . \quad (49)$$

Using also the expression for the derivative of the  $S$ -matrix in the narrow width limit (29) one can express the couplings in terms of quantities evaluated on the real axis

$$(\langle 0|j_S|S \rangle)^2 \simeq \frac{3}{16\pi} \sigma_\pi(M_S^2) M_S \Gamma_S \left( e^{-i\delta_0^0(M_S^2)} F_j(M_S^2) \right)^2 , \quad (50)$$

using  $\text{Re } z_S \simeq M_S^2$ ,  $\text{Im } z_S = M_S \Gamma_S$ . This expression shows that the squares of the couplings  $C_S^j$  must be real numbers in the narrow width limit, provided  $M_S$  is in the region of applicability of Watson's theorem. The couplings themselves can be either real or pure imaginary depending on whether the phase shift and the phase of the form-factor are equal or differ by  $\pi$ .

## 5.2 Numerical results

Analyticity and unitarity allows one to derive Omnès representations for the form-factors, analogous to those for the  $\gamma\gamma \rightarrow \pi\pi$  amplitude but much simpler because of the absence of a left-hand cut. Let us briefly recall the derivation. Let  $\overline{F}(s)$  be a two-component vector formed from the pion and kaon form-factors,

$${}^t \overline{F}(s) = (F_j^\pi(s), \frac{2}{\sqrt{3}} F_j^K(s)) \quad (51)$$

and multiply it with the inverse of the Omnès matrix<sup>8</sup>

$$\overline{G}(s) \equiv \mathbf{\Omega}^{-1}(s) \overline{F}(s) . \quad (52)$$

This multiplication removes part of the right-hand cut i.e. the components of  $\overline{G}(s)$  have a right-hand discontinuity which vanishes in the range

$$\text{Im } \overline{G}(s) \simeq 0, \quad 4m_\pi^2 \leq s \leq s_2 \quad (53)$$

where  $s_2$  is the point above which two-channel unitarity is no longer a good approximation. By construction, the components of  $\mathbf{\Omega}(s)$  behave as  $1/s$  when  $s \rightarrow \infty$  and a similar behaviour is expected from the form-factors, such that  $\overline{G}(s)$  should satisfy

---

<sup>8</sup>The determinant of the Omnès matrix can be expressed in analytical form:  $\det \mathbf{\Omega}(s) = \exp\left(\frac{s}{\pi} \int_{4m_\pi^2}^{\infty} ds' \frac{\phi(s')}{s'(s'-s)}\right)$  with  $\phi(s') = \theta(4m_K^2 - s') \delta_0^0(s') + \theta(s' - 4m_K^2) \delta_{\pi\pi \rightarrow K\bar{K}}(s')$  which shows that it does not vanish.

a once-subtracted dispersion relation. In terms of  $\bar{F}$ , it reads

$$\bar{F}(s) = \mathbf{\Omega}(s) \left[ \begin{pmatrix} \alpha \\ \beta \end{pmatrix} + \frac{s}{\pi} \int_{s_2}^{\infty} \frac{ds'}{s'(s'-s)} \text{Im} (\mathbf{\Omega}^{-1}(s') \bar{F}(s')) \right]. \quad (54)$$

In the range  $s \ll s_2$ , the energy dependence of the integral may be neglected and one ends up with the following representation for the form-factors

$$\begin{pmatrix} F_j^\pi(s) \\ \frac{2}{\sqrt{3}} F_j^K(s) \end{pmatrix} = \begin{pmatrix} \Omega_{11}(s) & \Omega_{12}(s) \\ \Omega_{21}(s) & \Omega_{22}(s) \end{pmatrix} \begin{pmatrix} \alpha + \alpha's \\ \beta + \beta's \end{pmatrix}. \quad (55)$$

As the discussion above shows, it is valid for  $s \ll s_2$ . Such representations were used and discussed in detail in ref. [46]. In order to determine the polynomial parameters, one can rely on chiral symmetry [46]. As a first approximation, one can use the chiral expansions of the form factors at order  $p^2$  and determine the polynomial coefficients by matching the  $O(p^2)$  values of  $F_j^P(0)$ ,  $\dot{F}_j^P(0)$  with those

$j_S$	$F_j^\pi(0)$	$\dot{F}_j^\pi(0)$	$F_j^K(0)$	$\dot{F}_j^K(0)$
$m_u \bar{u}u + m_d \bar{d}d$	$m_\pi^2$	0	$\frac{1}{2}m_\pi^2$	0
$m_s \bar{s}s$	0	0	$m_K^2 - \frac{1}{2}m_\pi^2$	0
$\theta_\mu^\mu$	$2m_\pi^2$	1	$2m_K^2$	1

Table 3: Pion and kaon form-factors associated with various operators  $j_S$ . The table shows their values at  $s = 0$  and the values of their derivatives at leading chiral order.

of the Omnès representation. These  $O(p^2)$  values are recalled in table 3. The representation (55) then allows one to compute the form-factors for complex values of  $s$  (with  $|s| < s_2$ ) and thus determine the values of the couplings between scalar operators and scalar mesons from residue relations like (45).

The numerical values of the absolute values of couplings (the phases will be shown later) of the  $\sigma$  and  $f_0(980)$  mesons to the  $\bar{q}q$  operators obtained in this manner are collected in table 4. In this table, the first error reflects the influence of higher order chiral corrections in the polynomial parameters. We have estimated that the order of magnitude, relative to the  $O(p^2)$  values, should be  $\simeq 30\%$  for the corrections proportional to  $m_s$ , and neglected the corrections proportional to  $m_{u,d}$ . As expected, a larger uncertainty is generated for the  $f_0(980)$  than for the  $\sigma$ . The second error is associated with the uncertainties in the  $\pi\pi$  and  $K\bar{K}$   $T$ -matrix as reflected in the Omnès matrix elements.

	$\sigma(600)$	$f_0(980)$
$ C_S^{uu} $ (MeV)	$206 \pm 4_{-6}^{+4}$	$82 \pm 31_{-7}^{+12}$
$ C_S^{ss} $ (MeV)	$17 \pm 5_{-7}^{+1}$	$146 \pm 44_{-7}^{+14}$

Table 4: Absolute values (in MeV) of the couplings of the  $\sigma$  and  $f_0(980)$  mesons to scalar  $\bar{q}q$  operators as defined in eq. (35).

A previous estimate of the  $\bar{q}q$  coupling of the  $\sigma$  meson, using Breit-Wigner approximations, was given in ref. [82] in the form  $\langle 0|\bar{d}d|\sigma\rangle = \sqrt{2/3}B_0/\chi$ , with  $\chi = 20 \text{ GeV}^{-1}$ , which is significantly smaller than our result. Some results for the couplings of the  $I = 1$  and  $I = 1/2$  mesons to  $\bar{q}q$  operators can be found in the literature. These resonances are reasonably narrow, such that various definitions should be equivalent and we can compare their values to those we found for the  $I = 0$  mesons. We normalise the couplings of these mesons in accordance with eq. (35)

$$\langle 0|\bar{u}s|K_0^*\rangle = B_0C_{K_0^*}^{us}, \quad \langle 0|\bar{u}d|a_0\rangle = B_0C_{a_0}^{ud}. \quad (56)$$

An evaluation of the  $a_0(980)$  coupling was performed in ref. [24] using finite-energy sum rules (see also ref. [83]). Converted to the normalisation of eq. (56), the result of [24] reads,

$$|C_{a_0(980)}^{ud}| = 197 \pm 37 \text{ MeV} \quad (57)$$

which is remarkably similar to the coupling of the  $\sigma$  meson  $C_\sigma^{uu}$  in table 4. The coupling  $C_{a_0(980)}^{ud}$  is related to the coupling  $c_m$  introduced in ref. [84] by  $C_{a_0(980)}^{ud} = 4c_m$  and can be estimated from its relation to the low-energy chiral coupling constants [84], eventually supplemented with large  $N_c$  or chiral sum rule constraints [85, 86]. These approaches yield values in the range  $C_{a_0(980)}^{ud} = [120, 200] \text{ MeV}$ . An unquenched lattice QCD calculation has also been performed [25] which gives:  $C_{a_0(980)}^{ud} = [304, 340] \text{ MeV}$ . These values should not be compared too literally to the preceding ones because they correspond to unphysical pion masses  $m_\pi/m_\pi^{\text{phys}} \gtrsim 5$  and only two dynamical flavours. An estimate for the  $\kappa$  meson coupling  $C_\kappa^{us}$  can be made following a similar approach to that used here for the  $\sigma$  meson. One can compute the position of the complex pole and the corresponding value of the  $S$ -matrix derivative from the Roy-Steiner equations [87]. The central values which one obtains in this way are

$$\sqrt{z_S} \simeq (658 + i277) \text{ MeV}, \quad \dot{S}_0^{\frac{1}{2}}(z_S) \simeq (0.59 + i2.03) \text{ GeV}^{-2} \quad (58)$$

The coupling can then be defined in terms of the  $K\pi$  scalar form-factor evaluated at  $z_S$  (see ref. [88], appendix C) and this gives

$$|C_{\kappa(800)}^{us}| \simeq 156 \text{ MeV}. \quad (59)$$

Comparing now the couplings of the  $I = 0$  mesons from table 4 to those of the  $I = 1, 1/2$  mesons one observes that the values of  $C_{\sigma}^{uu}$ ,  $C_{\kappa}^{us}$ ,  $C_{f_0(980)}^{ss}$ ,  $C_{a_0(980)}^{ud}$  are rather similar, the relative differences do not exceed  $\simeq 20\%$ . This is compatible with an assignment of the mesons  $\sigma$ ,  $\kappa$ ,  $f_0(980)$ ,  $a_0(980)$  into a nonet. Results on the couplings of the heavier scalar mesons  $a_0(1450)$  and  $K_0^*(1430)$  are also available. Ref. [24] gives

$$|C_{a_0(1450)}^{ud}| = 284 \pm 54 \text{ MeV}, \quad |C_{K_0^*(1430)}^{us}| = 370 \pm 20 \text{ MeV} . \quad (60)$$

The result for the  $a_0(1450)$  was obtained from a finite-energy sum rule and the one for the  $K_0^*(1430)$  from a one-channel Omnès representation. An evaluation using a two-channel representation and complex pole definition was made in ref. [88] which gives  $|C_{K_0^*(1430)}^{us}| \simeq 282 \text{ MeV}$ . With the normalisations used here, the couplings of the  $a_0(1430)$  and  $K_0^*(1430)$  to quark-antiquark operators seem to be significantly larger than those of the light scalars.

	$\sigma(600)$	$f_0(980)$
$ C_S^{\theta}  \text{ (MeV)}$	$197 \pm 15_{-6}^{+21}$	$114 \pm 44_{-7}^{+22}$
$ C_S^{GG}  \text{ (MeV)}$	$472 \pm 15_{-16}^{+26}$	$227 \pm 41_{-16}^{+51}$

Table 5: Absolute values of the couplings of the  $\sigma$  and  $f_0(980)$  to the gluonic operators  $\theta_{\mu}^{\mu}$  and  $\alpha_s G^2$ .

Finally, one can compute the couplings of the light  $I = 0$  scalars to the energy-momentum trace operator  $\theta_{\mu}^{\mu}$  using the chiral results for the associated form-factor at  $s = 0$  from table 3 . The results are shown on the first line of table 5. One finds that both the  $\sigma$  and the  $f_0(980)$  display a significant coupling to the  $\theta_{\mu}^{\mu}$  operator. The trace of the energy-momentum tensor has the following exact expression in QCD [93] with three heavy flavours integrated out

$$\theta_{\mu}^{\mu} = \frac{\beta(g)}{2g} G_{\mu\nu}^a G^{a\mu\nu} + (1 + \gamma_m(g)) \sum_{q=u,d,s} m_q \bar{q}q . \quad (61)$$

This expression allows one to disentangle the  $\alpha_s G^2$  part from the  $\bar{q}q$  one if one uses a perturbative approximation for the  $\beta$  function and for the anomalous dimension. The results shown in table 5 for  $C_S^{GG}$  correspond to a leading order approximation. Our results for  $C_S^{\theta}$  may be compared with the Laplace sum rule evaluation [8]

$$C_{\sigma}^{\theta} = [272, 329] \text{ MeV} . \quad (62)$$

However, one should keep in mind that in the calculation of [8], the spectral function  $\text{Im}\Pi_{jj}(s)$  corresponding to the operator  $j_S = \theta_\mu^\mu$  is approximated by a simple delta function. Fig. 5 shows our result for this spectral function based on using two-channel unitarity and physical  $\pi\pi$  scattering inputs. It displays a peak corresponding to the  $f_0(980)$  resonance, while the  $\sigma$  resonance does not show up as a clear enhancement, but generates a broadening of the  $f_0(980)$  peak at low energies. It is then plausible that the value (62) should be compared with the sum  $C_\sigma^\theta + C_{f_0}^\theta$  from table 5: the agreement is then rather reasonable.

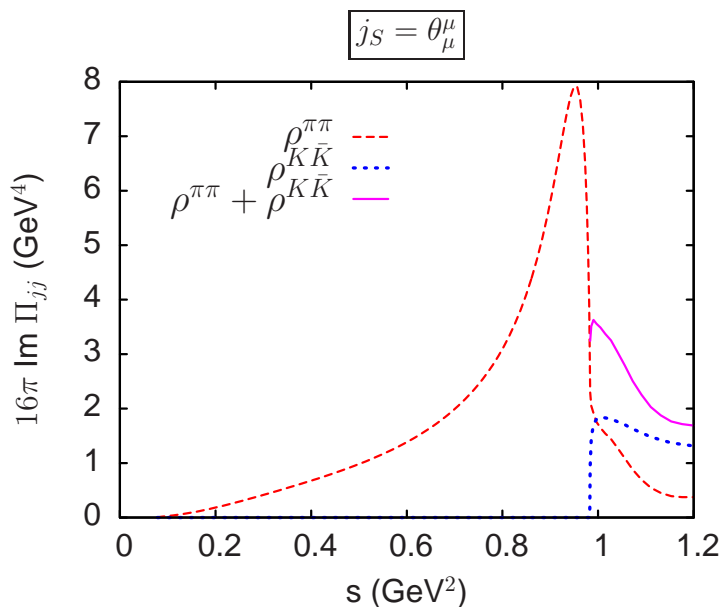


Figure 5: Spectral function of the  $\Pi_{jj}$  correlator with  $j_S = \theta_\mu^\mu$ . The long-dashed and short-dashed curves are the contributions from the  $\pi\pi$  and  $K\bar{K}$  intermediate states respectively.

Finally, the central values of the phases of the couplings  $C_S^j$  are shown in table 6. In the Breit-Wigner approximation, one expects the phases to be either zero or  $\pm 90^\circ$  (see (50)). The actual values are often not too different from this approximation.

## 6 Conclusions

We have considered several properties of the light scalar isoscalar mesons  $\sigma$  and  $f_0(980)$  using definitions which rely on the positions of the poles in the complex plane and their associated residues. This approach allows one to deal with a broad

	$\sigma$	$f_0(980)$
$\bar{u}u + \bar{d}d$	$28.2^\circ$	$89.1^\circ$
$\bar{s}s$	$-80.2^\circ$	$-14.2^\circ$
$\theta_\mu^\mu$	$87.2^\circ$	$-34.6^\circ$

Table 6: Central values of the phases of the couplings  $C_S^j$ .

resonance like the  $\sigma$  in a well defined way. In order to compute the positions of the poles and the residues, the Roy integral representation for the  $\pi\pi$  scattering amplitude  $t_0^0$  was used. On the real axis, we have started from the Roy equation solutions of ref. [38], which use a matching point  $\sqrt{s_m} = 0.8$  GeV and construct an extended solution which, for the  $S$ -wave  $t_0^0$ , has a higher matching point  $\sqrt{s_m} = 2m_K$  such as to improve the theoretical constraints on the  $f_0(980)$  meson properties. In order to constrain the value of the  $S$ -wave scattering phase-shift at the  $K\bar{K}$  threshold and discriminate between different shapes of the inelasticity, corresponding to different experiments, we perform fits of the phase-shifts below the  $K\bar{K}$  threshold based on the Roy solutions. We find that the solution corresponding to a deep-dip shaped inelasticity has a better  $\chi^2$  than that corresponding to a shallow-dip shape. This is in agreement with the observations of ref. [41]. The properties of the  $f_0(980)$  resonance, as expected, are particularly sensitive to the central value of the inelasticity. The results based on this Roy representation of the amplitude for the second-sheet pole positions are in table 2.

As a first application, we have re-determined the scalar to two photons couplings  $g_{S\gamma\gamma}$ , following the methodology first advocated in ref. [42], and based on the determinations of the  $\gamma\gamma \rightarrow \pi\pi$  amplitudes from the recent experimental measurements [43, 44]. The result found for the  $\sigma$  is somewhat smaller than that originally given in ref. [42]. As a second application, the couplings of the  $\sigma$  and  $f_0(980)$  mesons to scalar operators, which can be formally denoted as  $\langle 0|j_S(0)|\sigma\rangle$ ,  $\langle 0|j_S(0)|f_0(980)\rangle$  were defined and evaluated. Choosing  $j_S = (\bar{u}u + \bar{d}d)/\sqrt{2}$ ,  $j_S = \bar{s}s$  these matrix elements provide a quantitative measure of the quark-antiquark contents of the scalar mesons, while choosing  $j_S = \theta_\mu^\mu$  is a measure of the glue content. A simple, general relation can be established between such couplings and the value of the pion form-factor associated with the operator  $j_S$  computed at the position of the resonance pole,  $F_j^{\pi\pi}(z_S)$ . This relation is given in eq. (45) in the general case and in eq. (50) in the limiting case of a narrow resonance. Such form-factors are known to be calculable from a coupled-channel Omnès representation [46] which should be valid in a complex energy range which accomodates the  $\sigma$  as well as the  $f_0(980)$  resonances. The polynomial parameters in such representations are constrained by

chiral symmetry, for both the  $\bar{q}q$  and  $\theta_\mu^\mu$  operators, and can be estimated from the leading order chiral Lagrangian [46]. In principle, matrix elements of other types of operators, for instance tetraquark operators, could be addressed in the same way. The values of  $F_j(0)$  and  $\dot{F}_j(0)$ , in such cases, are not predicted from chiral symmetry but could be obtained e.g. from lattice QCD.

The numerical results for the  $\bar{q}q$  coupling constants of  $\sigma$  and the  $f_0(980)$  mesons are shown in table 4. The couplings are not particularly suppressed but it would be interesting to compare them with couplings to tetraquark operators. The couplings can also be compared to the analogous couplings of the  $I = 1$  and  $I = 1/2$  mesons to the  $\bar{u}d$  and  $\bar{u}s$  operators respectively for which estimates can be found in the literature including one calculation in lattice QCD [25]. This comparison supports a nonet assignment of the  $\sigma$ ,  $\kappa$ ,  $a_0(980)$ ,  $f_0(980)$  mesons. Our results for the couplings to the gluonic operators  $\theta_\mu^\mu$  and  $\alpha_s G^2$  indicate that both the  $\sigma$  and  $f_0(980)$  couple significantly to such operators as well.

## Acknowledgements

I would like to thank prof. W. Ochs for sending me original data tables and Martin Hoferichter for making several very useful comments on the manuscript.

## Appendix

We show below central values of the parameters of Roy solutions for the phase-shift  $\delta_0^0(s)$ , for a ten-parameter approximation according to eq. (11), corresponding to two different central values of the inelasticity function  $\eta_0^0$ , see sec. 2.

	$\eta_0^0$ : deep-dip	$\eta_0^0$ : shallow-dip
$s_0$	0.724237452	0.736126142
$\beta$	0.104114178	0.360170063
$\alpha_1$	0.140785825	0.146890648
$\alpha_2$	-0.0408980664	-0.0391129286
$\alpha_3$	0.00648917902	0.00545496306
$\alpha_4$	-0.000845352717	-0.000636406542
$\alpha_5$	$7.2010183310^{-5}$	$4.6272776510^{-5}$
$\alpha_6$	$-2.8956852410^{-6}$	$-8.8467901210^{-7}$
$\alpha_7$	$-8.9246247210^{-9}$	$-9.9351319610^{-8}$
$\alpha_8$	$3.0710899710^{-9}$	$4.8395284610^{-9}$

## References

- [1] S. K. Choi *et al.* [Belle Collaboration], Phys. Rev. Lett. **91** (2003) 262001 [arXiv:hep-ex/0309032], B. Aubert *et al.* [BABAR Collaboration], Phys. Rev. Lett. **95** (2005) 142001 [arXiv:hep-ex/0506081], S. K. Choi *et al.* [BELLE Collaboration], Phys. Rev. Lett. **100** (2008) 142001 [arXiv:0708.1790 [hep-ex]].
- [2] C. J. Morningstar and M. J. Peardon, Phys. Rev. D **60** (1999) 034509 [arXiv:hep-lat/9901004].
- [3] A. Hart *et al.* [ UKQCD Collaboration ], Phys. Rev. **D74** (2006) 114504. [hep-lat/0608026].
- [4] C. M. Richards, A. C. Irving, E. B. Gregory and C. McNeile [UKQCD Collaboration], Phys. Rev. D **82** (2010) 034501 [arXiv:1005.2473 [hep-lat]].
- [5] R. Frigori, C. Gattlinger, C. B. Lang, M. Limmer, T. Maurer, D. Mohler, A. Schafer, PoS **LAT2007** (2007) 114. [arXiv:0709.4582 [hep-lat]].
- [6] K. Hashimoto and T. Izubuchi, Prog. Theor. Phys. **119** (2008) 599 [arXiv:0803.0186 [hep-lat]].
- [7] V. A. Novikov, M. A. Shifman, A. I. Vainshtein and V. I. Zakharov, Nucl. Phys. B **165**, 67 (1980).
- [8] S. Narison and G. Veneziano, Int. J. Mod. Phys. A **4** (1989) 2751.
- [9] D. Harnett, R. T. Kleiv, K. Moats and T. G. Steele, Nucl. Phys. A **850** (2011) 110 [arXiv:0804.2195 [hep-ph]].
- [10] P. Minkowski and W. Ochs, Eur. Phys. J. C **9** (1999) 283 [arXiv:hep-ph/9811518].
- [11] C. Amsler, T. Gutsche, S. Spanier and N. A. Törnqvist, “Note on scalar mesons” in K. Nakamura *et al.* [Particle Data Group], J. Phys. G **37** (2010) 075021.
- [12] J. D. Weinstein and N. Isgur, Phys. Rev. D **41** (1990) 2236.
- [13] C. Hanhart, Yu. S. Kalashnikova, A. E. Kudryavtsev and A. V. Nefediev, Phys. Rev. D **75** (2007) 074015 [arXiv:hep-ph/0701214].
- [14] R. L. Jaffe, Phys. Rev. D **15** (1977) 267.
- [15] D. Black, A. H. Fariborz, F. Sannino and J. Schechter, Phys. Rev. D **59** (1999) 074026 [arXiv:hep-ph/9808415].

- [16] G. 't Hooft, Nucl. Phys. B **72** (1974) 461.
- [17] V. Cirigliano, G. Ecker, H. Neufeld and A. Pich, JHEP **0306** (2003) 012 [arXiv:hep-ph/0305311].
- [18] N. A. Törnqvist, Phys. Rev. Lett. **49** (1982) 624.
- [19] E. van Beveren, T. A. Rijken, K. Metzger, C. Dullemond, G. Rupp and J. E. Ribeiro, Z. Phys. C **30** (1986) 615 [arXiv:0710.4067 [hep-ph]].
- [20] J. R. Pelaez, Phys. Rev. Lett. **92** (2004) 102001 [arXiv:hep-ph/0309292].
- [21] P. Colangelo, F. De Fazio, F. Giannuzzi, F. Jugeau and S. Nicotri, Phys. Rev. D **78** (2008) 055009 [arXiv:0807.1054 [hep-ph]].
- [22] N. N. Achasov and V. N. Ivanchenko, Nucl. Phys. B **315** (1989) 465.
- [23] G. Amelino-Camelia *et al.*, Eur. Phys. J. C **68** (2010) 619 [arXiv:1003.3868 [hep-ex]].
- [24] K. Maltman, Phys. Lett. B **462** (1999) 14 [arXiv:hep-ph/9906267].
- [25] C. McNeile and C. Michael [UKQCD Collaboration], Phys. Rev. D **74** (2006) 014508 [arXiv:hep-lat/0604009].
- [26] S. Prelovsek, T. Draper, C. B. Lang, M. Limmer, K. F. Liu, N. Mathur and D. Mohler, Phys. Rev. D **82** (2010) 094507 [arXiv:1005.0948 [hep-lat]].
- [27] K. Jansen, C. McNeile, C. Michael, C. Urbach, Phys. Rev. D **80** (2009) 054510 [arXiv:0906.4720 [hep-lat]].
- [28] I. Caprini, G. Colangelo and H. Leutwyler, Phys. Rev. Lett. **96** (2006) 132001 [arXiv:hep-ph/0512364].
- [29] S. M. Roy, Phys. Lett. B **36** (1971) 353.
- [30] M. R. Pennington and S. D. Protopopescu, Phys. Rev. D **7** (1973) 1429.
- [31] J. L. Basdevant, C. D. Froggatt and J. L. Petersen, Nucl. Phys. B **72** (1974) 413.
- [32] S. Pislak *et al.* [BNL-E865 Collaboration], Phys. Rev. Lett. **87** (2001) 221801 [arXiv:hep-ex/0106071].
- [33] J. R. Batley *et al.* [NA48/2 Collaboration], Phys. Lett. B **633** (2006) 173 [arXiv:hep-ex/0511056], J. R. Batley *et al.*, Eur. Phys. J. C **64** (2009) 589.

- [34] B. Adeva *et al.* [DIRAC Collaboration], Phys. Lett. B **619** (2005) 50 [arXiv:hep-ex/0504044].
- [35] J. R. Batley *et al.* [NA48/2 Collaboration], Eur. Phys. J. C **54** (2008) 411.
- [36] J. R. Batley *et al.* [NA48-2 Collaboration], Eur. Phys. J. C **70** (2010) 635.
- [37] B. Ananthanarayan and P. Büttiker, Phys. Rev. D **54** (1996) 1125 [arXiv:hep-ph/9601285].
- [38] B. Ananthanarayan, G. Colangelo, J. Gasser and H. Leutwyler, Phys. Rept. **353** (2001) 207 [arXiv:hep-ph/0005297].
- [39] S. Descotes-Genon, N. H. Fuchs, L. Girlanda and J. Stern, Eur. Phys. J. C **24** (2002) 469 [arXiv:hep-ph/0112088].
- [40] R. Kaminski, J. R. Pelaez and F. J. Yndurain, Phys. Rev. D **77** (2008) 054015 [arXiv:0710.1150 [hep-ph]].
- [41] R. Garcia-Martin, R. Kaminski, J. R. Pelaez, J. Ruiz de Elvira and F. J. Yndurain, Phys. Rev. D **83** (2011) 074004 [arXiv:1102.2183 [hep-ph]].
- [42] M. R. Pennington, Phys. Rev. Lett. **97** (2006) 011601.
- [43] T. Mori *et al.* [Belle Collaboration], J. Phys. Soc. Jap. **76** (2007) 074102 [arXiv:0704.3538 [hep-ex]].
- [44] S. Uehara *et al.* [Belle Collaboration], Phys. Rev. D **78** (2008) 052004 [arXiv:0805.3387 [hep-ex]].
- [45] R. Garcia-Martin and B. Moussallam, Eur. Phys. J. C **70** (2010) 155 [arXiv:1006.5373 [hep-ph]].
- [46] J. F. Donoghue, J. Gasser, H. Leutwyler, Nucl. Phys. **B343**, 341-368 (1990).
- [47] C. Pomponiu and G. Wanders, Nucl. Phys. B **103** (1976) 172.
- [48] D. Atkinson and R. L. Warnock, Phys. Rev. D **16** (1977) 1948.
- [49] J. Gasser and G. Wanders, Eur. Phys. J. C **10** (1999) 159 [arXiv:hep-ph/9903443].
- [50] A. Schenk, Nucl. Phys. B **363** (1991) 97.
- [51] J. J. Moré, B. S. Garbow, and K. E. Hillstom, User Guide for MINPACK-1, Argonne National Laboratory Report ANL-80-74, Argonne, Ill., 1980.

- [52] D. H. Cohen, D. S. Ayres, R. Diebold, S. L. Kramer, A. J. Pawlicki and A. B. Wicklund, Phys. Rev. D **22** (1980) 2595.
- [53] A. Etkin *et al.*, Phys. Rev. D **25** (1982) 1786.
- [54] S. J. Lindenbaum and R. S. Longacre, Phys. Lett. B **274** (1992) 492.
- [55] D. Morgan and M. R. Pennington, Phys. Rev. D **48** (1993) 1185.
- [56] D. V. Bugg, B. S. Zou and A. V. Sarantsev, Nucl. Phys. B **471** (1996) 59.
- [57] D. Alde *et al.* [Serpukhov-Brussels-Los Alamos-Anneecy(LAPP) Collaboration], Nucl. Phys. B **269** (1986) 485.
- [58] B. Hyams *et al.*, Nucl. Phys. B **64** (1973) 134.
- [59] R. Kaminski, L. Lesniak and K. Rybicki, Z. Phys. C **74** (1997) 79 [arXiv:hep-ph/9606362].
- [60] P. Estabrooks and A. D. Martin, Nucl. Phys. B **79** (1974) 301.
- [61] W. Ochs, PiN Newslett. **3** (1991) 25.
- [62] S. D. Protopopescu *et al.*, Phys. Rev. D **7** (1973) 1279.
- [63] Z. Xiao and H. Q. Zheng, Commun. Theor. Phys. **48** (2007) 685 [arXiv:hep-ph/0103042].
- [64] R. Omnès, Nuovo Cim. **8** (1958) 316.
- [65] O. Babelon, J. L. Basdevant, D. Caillerie, M. Gourdin and G. Mennessier, Nucl. Phys. B **114** (1976) 252.
- [66] Y. Mao, X. G. Wang, O. Zhang, H. Q. Zheng and Z. Y. Zhou, Phys. Rev. D **79** (2009) 116008 [arXiv:0904.1445 [hep-ph]].
- [67] N. I. Muskhelishvili, “Singular Integral Equations”, *P. Noordhoff, Groningen (1953)*
- [68] J. Gasser, M. A. Ivanov and M. E. Sainio, Nucl. Phys. B **728** (2005) 31 [arXiv:hep-ph/0506265].
- [69] J. Gasser, M. A. Ivanov and M. E. Sainio, Nucl. Phys. B **745** (2006) 84 [arXiv:hep-ph/0602234].
- [70] M. R. Pennington, Phys. Rev. Lett. **97** (2006) 011601.

- [71] J. A. Oller, L. Roca and C. Schat, Phys. Lett. B **659** (2008) 201 [arXiv:0708.1659].
- [72] M. R. Pennington, T. Mori, S. Uehara and Y. Watanabe, Eur. Phys. J. C **56** (2008) 1 [arXiv:0803.3389].
- [73] J. Bernabeu and J. Prades, Phys. Rev. Lett. **100** (2008) 241804 [arXiv:0802.1830 [hep-ph]].
- [74] G. Mennessier, S. Narison and W. Ochs, Phys. Lett. B **665** (2008) 205 [arXiv:0804.4452 [hep-ph]].
- [75] Y. Mao, X. G. Wang, O. Zhang, H. Q. Zheng and Z. Y. Zhou, Phys. Rev. D **79** (2009) 116008 [arXiv:0904.1445 [hep-ph]].
- [76] G. Mennessier, S. Narison and X. G. Wang, Phys. Lett. B **696** (2011) 40 [arXiv:1009.2773 [hep-ph]].
- [77] M. Hoferichter, D. R. Phillips and C. Schat, arXiv:1106.4147 [hep-ph].
- [78] N. N. Achasov and G. N. Shestakov, Phys. Rev. D **77** (2008) 074020 [arXiv:0712.0885 [hep-ph]].
- [79] L. V. Fil'kov and V. L. Kashevarov, Eur. Phys. J. A **5** (1999) 285 [arXiv:nucl-th/9810074].
- [80] K. Nakamura *et al.* [Particle Data Group], J. Phys. G **37** (2010) 075021.
- [81] C. Itzykson and J. B. Zuber, “Quantum Field Theory,” *McGraw-Hill, New-York (1980)*
- [82] S. Gardner and U. G. Meißner, Phys. Rev. D **65** (2002) 094004 [arXiv:hep-ph/0112281].
- [83] S. Narison, Riv. Nuovo Cim. **10N2** (1987) 1.
- [84] G. Ecker, J. Gasser, A. Pich and E. de Rafael, Nucl. Phys. B **321** (1989) 311.
- [85] M. Jamin, J. A. Oller and A. Pich, Nucl. Phys. B **622** (2002) 279 [arXiv:hep-ph/0110193].
- [86] I. Rosell, J. J. Sanz-Cillero and A. Pich, JHEP **0701** (2007) 039 [arXiv:hep-ph/0610290].
- [87] S. Descotes-Genon and B. Moussallam, Eur. Phys. J. C **48** (2006) 553 [arXiv:hep-ph/0607133].

- [88] B. El-Bennich, A. Furman, R. Kaminski, L. Lesniak, B. Loiseau and B. Mous-sallam, Phys. Rev. D **79** (2009) 094005 [Erratum-ibid. D **83** (2011) 039903] [arXiv:0902.3645 [hep-ph]].
- [89] U. G. Meißner and J. A. Oller, Nucl. Phys. A **679** (2001) 671 [arXiv:hep-ph/0005253].
- [90] J. Bijnens and P. Dhonte, JHEP **0310** (2003) 061 [arXiv:hep-ph/0307044].
- [91] J. F. Donoghue, H. Leutwyler, Z. Phys. **C52**, 343-351 (1991).
- [92] J. Bijnens and I. Jemos, arXiv:1103.5945 [hep-ph].
- [93] J. C. Collins, A. Duncan and S. D. Joglekar, Phys. Rev. D **16** (1977) 438.
- [94] N. K. Nielsen, Nucl. Phys. B **120** (1977) 212.